Lawrence Berkeley National Laboratory
Recent Work

Title
Calibration and Performance of the Mark II Drift Chamber Vertex Detector

Permalink
https://escholarship.org/uc/item/3dw364jh

Author
Durrett, D.

Publication Date
1990-05-01

eScholarship.org Powered by the California Digital Library
University of California

UC-414
LBL-29108

Lawrence Berkeley Laboratory
UNIVERSITY OF CALIFORNIA

Physics Division

Presented at the Fifth International Conference on
Instrumentation for Colliding Beam Physics,
Novosibirsk, USSR, March 15–21, 1990, and
to be published in the Proceedings

Calibration and Performance of the Mark II Drift Chamber Vertex Detector

D. Durrett *et al.*

May 1990

For Reference

Not to be taken from this room

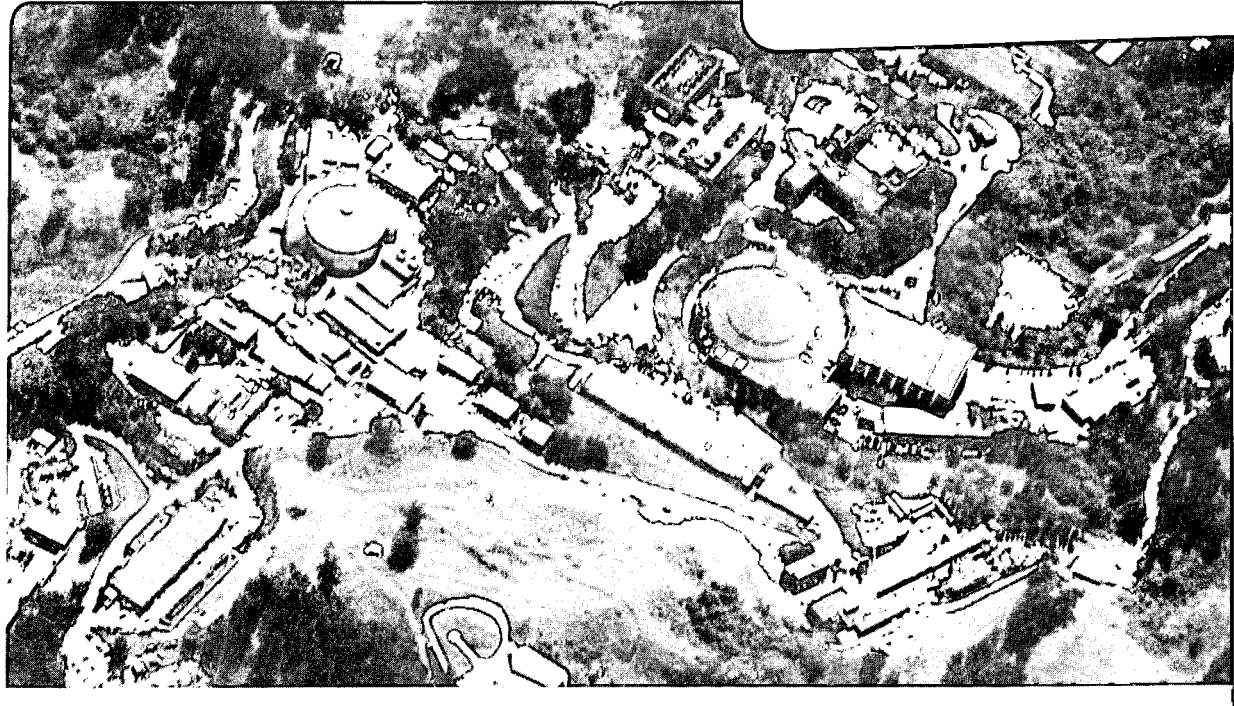

LBL-29108
Copy 1
Bldg. 50 Library.

Prepared for the U.S. Department of Energy under Contract Number DE-AC03-76SF00098.

DISCLAIMER

This document was prepared as an account of work sponsored by the United States Government. While this document is believed to contain correct information, neither the United States Government nor any agency thereof, nor the Regents of the University of California, nor any of their employees, makes any warranty, express or implied, or assumes any legal responsibility for the accuracy, completeness, or usefulness of any information, apparatus, product, or process disclosed, or represents that its use would not infringe privately owned rights. Reference herein to any specific commercial product, process, or service by its trade name, trademark, manufacturer, or otherwise, does not necessarily constitute or imply its endorsement, recommendation, or favoring by the United States Government or any agency thereof, or the Regents of the University of California. The views and opinions of authors expressed herein do not necessarily state or reflect those of the United States Government or any agency thereof or the Regents of the University of California.

SLAC-PUB-5259
LBL-29108
May 1990
(E/I)

CALIBRATION AND PERFORMANCE OF THE MARK II DRIFT CHAMBER VERTEX DETECTOR*

D. DURRETT, W. T. FORD, D. A. HINSHAW, P. RANKIN,
J. G. SMITH, and P. WEBER
Department of Physics, University of Colorado,
Boulder, CO 80309, USA

J. F. KRAL, B. A. SCHUMM, and G. H. TRILLING
Lawrence Berkeley Laboratory and Department of Physics
University of California, Berkeley, CA 94720, USA

and

D. FUJINO, K. HAYES,‡ J. A. JAROS, D. S. KOETKE,
L. A. KOWALSKI, C. T. MUNGER, and S. R. WAGNER
Stanford Linear Accelerator Center,
Stanford University, Stanford, CA 94309, USA

ABSTRACT

We have calibrated and studied the performance of the MARK II drift chamber vertex detector with cosmic ray tracks collected with the chamber inside the MARK II detector at the SLC. The chamber achieves 30 μm impact parameter resolution and 500 μm track-pair resolution using CO_2/C_2H_6 (92/8) at 2 atmospheres pressure. The chamber has successfully recorded Z^0 decays at the SLC, and resolved tracks in dense hadronic jets with good efficiency and high accuracy.

* Work supported by Department of Energy contract DE-AC03-76SF00515 (SLAC), DE-AC02-86ER40253 (Colorado), and DE-AC03-76SF00098 (LBL).
‡ Present address: Physics Dept., Hillsdale College, Hillsdale, MI 49292, USA.

Invited talk presented at the Vth International Conference on Instrumentation for Colliding Beam Physics, Novosibirsk, USSR, March 15-21, 1990.

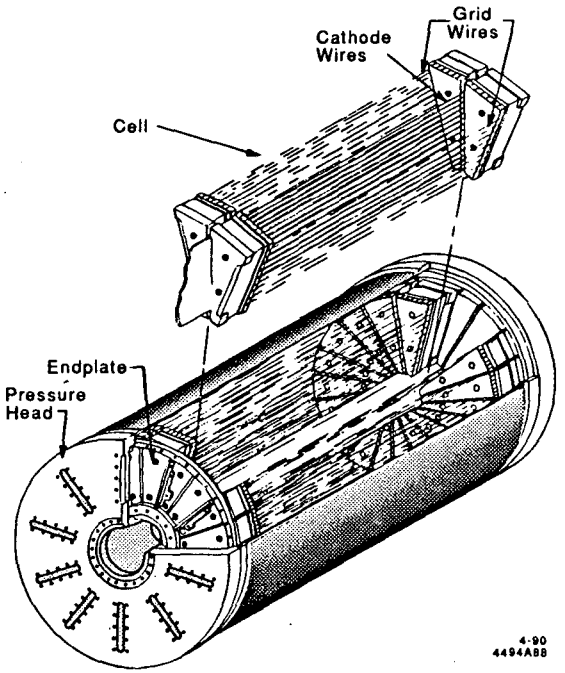

Figure 1: MARK II drift chamber vertex detector, showing the modular construction of the jet cells and the pressure vessel.

1. Introduction

The use of "cool" gases in drift chambers permits significant improvements in spatial and double track resolution[1] and has prompted several groups to explore the technique for use in precision tracking chambers and vertex detectors. Spatial resolution is improved because the electron diffusion is near its (thermal) lower limit. Typical drift velocities in cool gas chambers are roughly an order of magnitude slower than in "fast" gases, simplifying the electronic problems associated with resolving closely spaced tracks and leading to improved double track resolution. On the other hand, since the drift velocity is linearly proportional to the reduced field E/P, any non-uniformities in the drift field complicate the distance-time relation. In addition, since the drift velocity depends on the temperature, pressure, and gas composition, control of all these parameters is required to maintain a stable calibration.

The MARK II Drift Chamber Vertex Detector[2] (DCVD) is a high precision pressurized drift chamber which has just been installed as part of the vertex detector system for the MARK II detector[3] at the Stanford Linear Collider. The

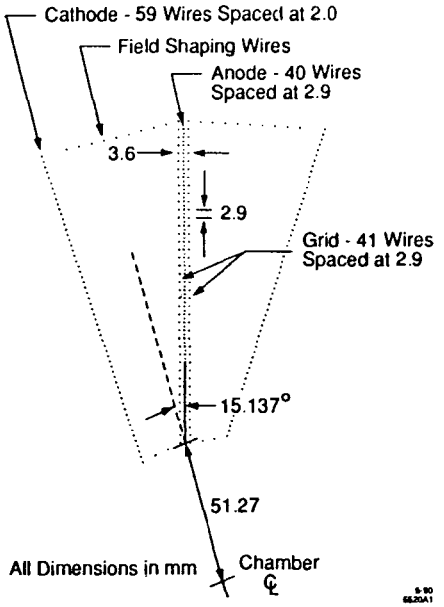

Figure 2: Wire placements in one jet cell.

chamber uses a cool gas, CO_2/C_2H_6 (92/8), and operates at 2 atm pressure. During the past year we have taken cosmic ray data with the MARK II detector in order to study the chamber's performance, calibrate its distance-time relation, and determine its alignment with respect to the MARK II central tracking chamber. In January 1990 the chamber was used to record Z^0 decays at the SLC. This paper reviews the procedures followed in calibrating the chamber, summarizes its present level of performance, and demonstrates that cool gas chambers can operate near design performance.

2. Chamber Description

The DCVD is a jet-type drift chamber divided into 10 axial drift cells (see Fig. 1). Individual cells are tilted with respect to the radial direction to resolve the left-right ambiguity, to ensure that no track is poorly measured along its entire length, and to help in drift velocity calibration. A jet cell is shown in Fig. 2. There are 38 active anode wires, 55 cm long, positioned at radii between roughly 5 and 17 cm. Sense-field wire planes are sandwiched between grid wire planes. The latter focus incoming electrons onto the anodes and improve the charge collection isochrony. The sense to field spacing was made rather small (1.45 mm) to improve the double track

resolution. Extra electrodes at the innermost and outermost radii minimize edge effects. The chamber is read out with a fast integrating preamplifier, the output of which is shaped, amplified further, and transmitted to a 6 bit 100 MHz FADC, 1024 buckets deep. Details of the chamber construction, electronics, and chamber subsystems can be found in Ref. 3.

Our philosophy in designing the chamber was to make an electrostatic structure that could be described with as few parameters as possible. To this end, wires in the chamber were accurately located in planes, so that only coordinates describing the location of the plane, and not the individual wire positions, are needed for chamber calibration. RMS deviations of anode wire positions out of the plane are < 3 μm. The wire planes are positioned with an accuracy ~ 20 μm. Care was also taken to provide accurate high voltage distribution. Ten resistor divider chains, one for each cell, supply the 68 voltages required for the cathode and field-shaping electrodes, accurate to better than 0.1%.

Chamber temperature, pressure, and high voltage are closely controlled in order to stabilize the drift velocity. Over a one-month run, the chamber pressure was maintained with a commercial pressure transducer/controller at 2 atmospheres and was stable to about 0.03%. Chamber temperature was maintained at $28.15° \pm 0.05°$C by circulating temperature-controlled water through 6 mm diameter aluminum tubing that was soldered to the inner and outer radii of the pressure heads and welded in a spiral around the outer shell of the chamber. The inner Beryllium core of the chamber was not actively controlled and showed $\pm 0.15°$C temperature excursions which coincided with environmental temperature changes. The maximum temperature difference between the inner core and the outer shell was less than 0.35°C. The chamber gas was premixed in a quantity sufficient for one year of chamber operation, which guaranteed that the composition was stable. High voltages were monitored during running. The cathode supply was stable to 0.03% over a period of a month; the anode supplies were stable to 0.3%.

3. Distance-Time Relation

At our typical drift field of 0.73 kV/cm/atm, the measured drift velocity is 5.6 μm/ns, while in the high fields near the sense wires, the drift velocity becomes 100 μm/ns or greater. We determine the distance-time relation near the anode by first calculating the electric field along lines perpendicular to the sense-field plane which intersect the sense wire, using a superposition of solutions corresponding to an array of infinite wire planes.[4] The field is given by

$$E(d) = \frac{2\pi}{a}\left\{Q_S \coth\frac{\pi d}{a} + Q_F \tanh\frac{\pi d}{a} + Q_G\left(\tanh\frac{\pi(d+b)}{a} + \tanh\frac{\pi(d-b)}{a}\right)\right\},$$

where Q_S, Q_F, and Q_G are, respectively, the charges per unit length on the sense, field, and grid wires; a is the spacing between sense wires, b is the distance from

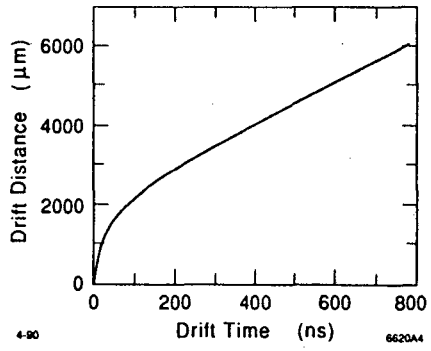

Figure 3: The distance-time relation near the sense wire.

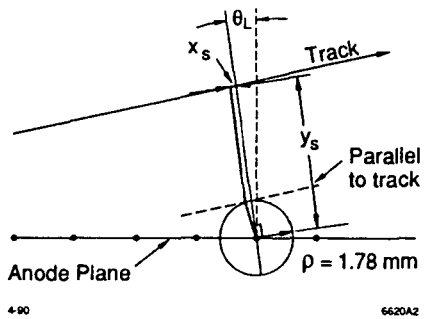

Figure 4: Electron drift trajectory for tracks which are not parallel to the sense plane.

the sense/field plane to the grid plane, and d is the distance from the sense wire. A detailed electrostatics simulation of the drift chamber indicates that this formula describes the field at all drift distances with 0.1% accuracy for sense wires near the center of the jet cell. Thus we have a convenient first-order electrostatics model.

We combine this model with a function relating drift velocity to electric field, derived from measurements in pure CO_2.[5] For our mixture of CO_2 with 8% ethane, we scale all drift velocities up by the factor of 1.1 in order to reproduce the measured velocity far from the grid. The resulting relationship between drift distance and drift time is shown in Fig. 3. For drift distances greater than 6 mm, the first-order model assumes a constant drift velocity.

For tracks which are not parallel to the sense plane, we assume that electrons follow a path which is perpendicular to the sense plane until they are within a radius of 1.78 mm of the sense wire, at which point they drift radially (see Fig. 4). This radius is determined from the electrostatics simulation to match the radius of

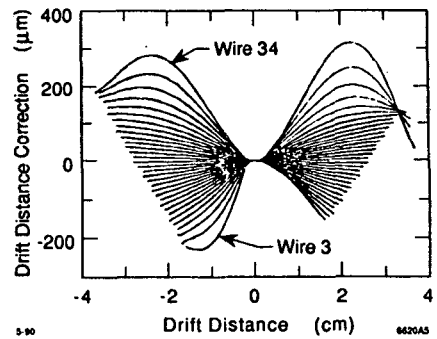

Figure 5: Corrections applied to the first-order model, derived from an electrostatic simulation of the jet cell. The corrections are given for wires number 3 through 34 vs. drift distance.

curvature of lines of constant drift time. The same distance-time relation is applied, but the distance is now taken to be the length of this modified trajectory. For all tracks, a Lorentz angle correction due to the 0.475 T magnetic field tilts the drift trajectory by 18.2 mrad. This is the calculated Lorentz angle and studies show it to be appropriate for our gas to within about 20%.

In order to account for edge effects and a small radial dependence of the electric field, we use a full electrostatics simulation to determine corrections to the first-order model as a function of drift distance and layer number, again only along a line passing through the sense wire. For each 2 mm interval in drift distance and each of the 38 layers of the chamber, we calculate a deviation from the first-order electric field. This correction is integrated in order to determine a drift distance correction for any point in the chamber. The corrections are shown in Fig. 5. A further small correction is implemented for angled tracks, to account for field distortions near the grid wires. This correction is calculated from the electrostatics program for angles up to 30 degrees and distances from 0 to 4 mm.

Finally, we have refined the distance-time relation empirically by studying residuals from best fit tracks using a sample of cosmic rays. This correction is described in the following section.

4. Tracking Performance

a. Data Sets and Track Reconstruction

The vertex detector was operated in a 0.475 T solenoidal magnetic field, surrounded by the MARK II main drift chamber and trigger scintillators. The main chamber and its pattern recognition programs were well understood from prior experience at PEP. Tracks measured in the main chamber are extrapolated into the

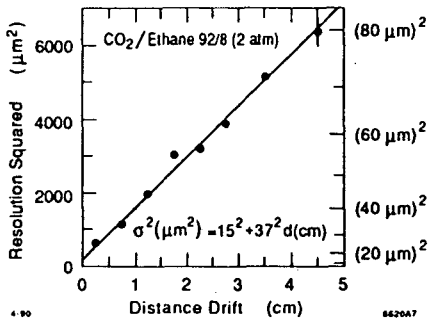

Figure 6: Resolution per layer vs. drift distance.

vertex chamber volume to guide the search for matching measurements in the vertex chamber. Fits to the combined sets of measurements from both detectors establish the direction and momentum of each track, treated as if it originated near the center of the detector and propagated outward. With each cosmic ray yielding two tracks that were known a priori to be parts of a single trajectory, we studied the agreement of the two independent impact parameters (miss distance) and directions (acoplanarity) to optimize both the internal calibration of the vertex detector and its alignment with the main chamber.

b. Resolution vs. Drift Distance

We determine the local resolution by measuring the rms tracking residuals as a function of drift distance (Fig. 6). The resolution shows the expected proportionality to the square root of drift distance caused by diffusion of the ionization electrons. These data show that the resolution is 25–80 μm in our range of drift distances, averaging around 50 μm. Near the anode, the resolution is worse because of the large, rapidly varying drift velocity, and because the random spacing between primary electron clusters becomes a significant contribution to drift distance. The distribution of track residuals near the anode is shown in Fig. 7. For the same reasons but to a much lesser extent, the region close to the cathode has degraded resolution. The tilt of the jet cell minimizes the effect of these low resolution regions on the cell's impact parameter resolution. Figure 8 shows the impact parameter resolution calculated on the basis of actual hit patterns and resolution per hit for a cosmic ray sample. The response is fairly uniform across the cell.

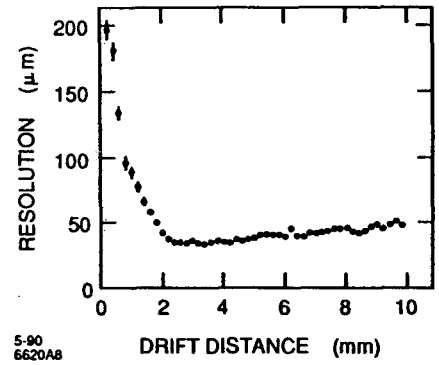

Figure 7: Resolution per layer vs. drift distance near the anode.

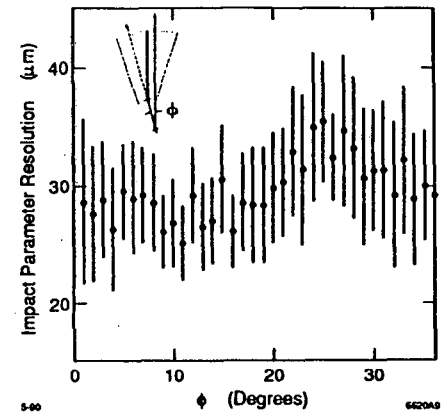

Figure 8: Calculated impact parameter resolution vs. azimuthal track angle with respect to the jet cell for cosmic rays with $p > 5$ GeV/c.

c. Systematic Corrections

The accuracy with which tracks can be extrapolated to the production point depends upon our ability to correct for distortions throughout the entire drift cell. Guided by studies of the miss distance and acoplanarity of cosmic ray half-track pairs, we have found that distortions remain after we apply the corrections based upon the model of electron drift discussed in the previous section. We parameterize a correction to the distance-time function to third order in each of the two spatial

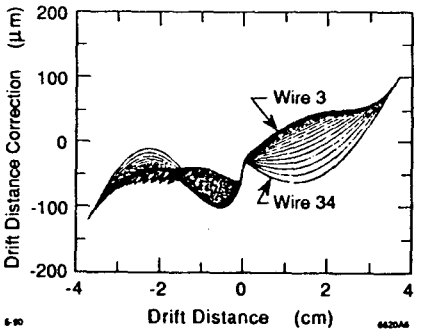

Figure 9: Empirical corrections applied to the first-order distance-time relation, given for wires number 3 through 34 vs. drift distance.

dimensions, i.e., signed drift distance and $(w - 19)$, where the wire number w runs from small to large radii.

These parameters together with the drift velocity scale and drift time offset (22 parameters altogether) are determined from a fit to a sample of about 600 cosmic rays. For this purpose the individual cosmic rays are fit in the vertex chamber alone as single tracks. We require each track to have momentum at least 5 GeV/c and to pass within 2.5 cm of the chamber axis. The first two and last four wires of each jet cell are excluded, as are measurements within 1 mm of either the sense wire or cathode plane. There must be at least 45 measurements (of 64 possible). Residuals greater than 180 μm are excluded from these parameter fits. The resulting empirical corrections are shown in Fig. 9. The curves show that effects not accounted for by the model distort the measurements by less than 50 μm except for a few outer wires on one side in the jet cell.

d. Impact Parameter Resolution

The distribution of cosmic half-track pair miss distances with the corrections described above is presented in Fig. 10. The Gaussian fit to these data gives 44 μm for the standard deviation, or 31 μm for the impact parameter resolution. This is about 30% larger than we find by propagating the local resolution measured by Fig. 6. This excess must be accounted for by systematic effects which are not yet understood.

At this writing we have a small sample of Z^0 decay events. This includes two Bhabha events; these have miss distances well within the resolution we measure with cosmic rays. The distribution of residuals seen in hadronic events is about 10% worse than that seen in cosmic ray events because of the presence of background hits in the chamber.

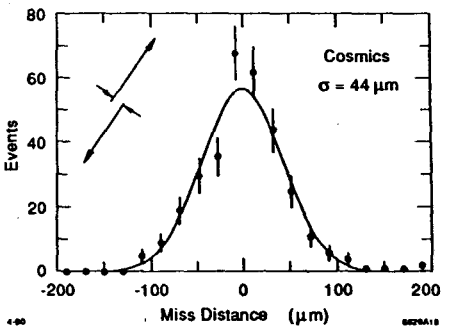

Figure 10: Distribution of miss-distances for cosmic rays with $p > 15$ GeV/c.

5. Double Track Resolution

Good double track resolution is essential for precision tracking in hadronic decays of the Z^0. It permits closely spaced tracks to be resolved close to the interaction point, and it provides good pattern recognition capability even in the presence of backgrounds.

The ability to distinguish two closely spaced tracks is limited by the late arrival of charge clusters from the first hit. Late-arriving clusters are created close to the boundary between the drift regions of adjacent anode wires. They have comparatively longer drift paths and pass through regions of lower electric field strength than clusters produced near the center of the drift region, and so they experience a significant delay in arriving at the anode. These clusters tend to broaden the pulse, or if delayed long enough, to appear as a second, distinct pulse. Although such second ("fake") pulses tend to be smaller than those caused by the primary ionization in the center of the drift region, fluctuations in the ionization and avalanche gain processes often make these pulses indistinguishable from those of a closely spaced second track.

The pattern recognition algorithm used for hit finding has been optimized to provide the best suppression of fake hits while maintaining a single hit efficiency in excess of 98%. The algorithm steps through the digitized pulse train bin by bin, forming the difference between the sum of three adjacent bins and the sum of the three succeeding bins. A leading edge is flagged if this difference exceeds a threshold, which decreases with drift distance according to $T \propto (1 - 0.08d)$, where d is given in cm, in order to compensate for the effects of diffusion and pulse height attenuation. A trailing edge is flagged when the difference of sums is negative for two consecutive bins. In order to discriminate further against the smaller fake hits, the pulse is ignored if its total pulse height between leading and trailing edges is less than a second drift-distance dependent threshold.

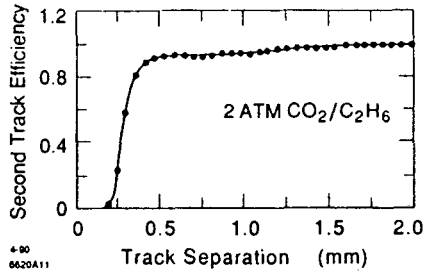

Figure 11: Efficiency to detect a second track as a function of track separation.

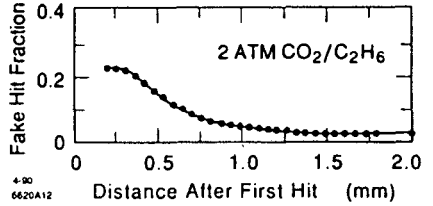

Figure 12: Fraction of "fake" hits as a function of distance after the first hit.

The double track resolution has been studied by superposing the pulse trains from different cosmic ray events, and measuring the efficiency of finding the second hit as the separation between the superposed hits is increased. These results are shown in Fig. 11 and show nearly full efficiency at separations as small as 400 μm. The slight loss in efficiency for tracks separated less than 1500 μm occurs because the presence of the first pulse occasionally perturbs the arrival time of the second pulse by a small amount. The fake hit rate has been studied with isolated tracks from cosmic ray data. Figure 12 shows the probability of detecting a fake hit beyond a given distance from the first hit as a function of that distance. The fake hit rate drops below 10% beyond 700 μm after the first hit. The double track resolution has also been studied in a limited sample of Z^0 decays, where the presence of closely spaced tracks is determined by extrapolating tracks from MARK II's central tracking chamber into the DCVD. The result is compatible with the cosmic ray study discussed above.

Figure 13 shows a Z^0 decay recorded during a test run at the SLC in January 1990. Cathode planes are shown by dashed lines in the figure. Anode planes are midway between cathode planes. Hits are plotted with their ambiguities, giving rise to patterns which are symmetric about the anode planes. Solid lines represent tracks extrapolated from the central tracking chamber. The dominant SLC backgrounds are soft, looping tracks which are apparent in the figure. Hadronic tracks stand out even in the presence of the backgrounds.

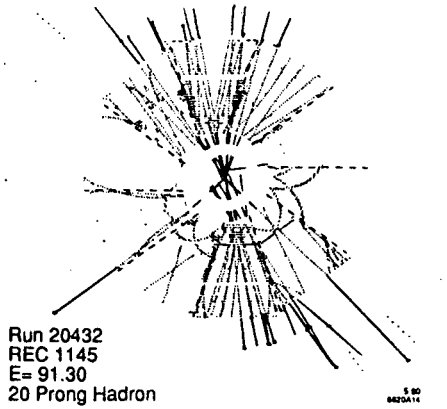

Figure 13: Hadronic decay of a Z^0 recorded in the drift chamber vertex detector.

6. Conclusions

The MARK II drift chamber vertex detector has been calibrated with a sample of cosmic ray data taken with the entire MARK II detector. Stable drift velocities were achieved by careful control of the chamber temperature, gas pressure and composition, and chamber high voltage. The impact parameter resolution for high momentum tracks is 30 μm. Two tracks can be efficiently resolved if they are separated by more than 500 μm. The chamber has successfully recorded Z^0 decays in a brief checkout run at the Stanford Linear Collider and efficiently tracks dense hadronic jets in the presence of machine-related backgrounds.

7. Acknowledgements

We thank the technicians and staff of the Lawrence Berkeley Laboratory and Stanford Linear Accelerator Center with whom we worked to design, build, test, and install the MARK II drift chamber vertex detector. We acknowledge our colleagues in the MARK II Collaboration for their help and support in installing, debugging, and operating the vertex drift chamber.

References

1. S. Bobkov et al., *Nucl. Instr. and Meth.* **226** (1984) 355; V. Commichau et al., *Nucl. Instr. and Meth.* **A235** (1985) 267; D. Bettoni et al., *Nucl. Instr. and Meth.* **A236** (1985) 237.
2. J. P. Alexander et al., *Nucl. Instr. and Meth.* **A283** (1989) 519.

3. G. S. Abrams et al., *Nucl. Instr. and Meth.* **A281** (1989) 55.

4. G. A. Erskine, *Nucl. Instr. and Meth.* **105** (1972) 565.

5. M. T. Elford, *Aust. J. Phys.* **19** (1966) 629; R. A. Sierra, H. L. Brooks, and K. J. Nygaard, *Appl. Phys. Lett.* **35** (1979) 764.

LAWRENCE BERKELEY LABORATORY
UNIVERSITY OF CALIFORNIA
INFORMATION RESOURCES DEPARTMENT
BERKELEY, CALIFORNIA 94720